 CMC, vol.13, no.2, pp.89-113, 2009

Modeling of Moisture Diffusion in Heterogeneous Epoxy Resin Containing Multiple Randomly Distributed Particles Using Hybrid Moisture Element Method

De-Shin Liu[1], Zhen-Wei Zhuang[1,2] Cho-Liang Chung[3] and Ching-Yang Chen[4]

Abstract: This paper employs a novel numerical technique, designated as the hybrid moisture element method (HMEM), to model and analyze moisture diffusion in a heterogeneous epoxy resin containing multiple randomly distributed particles. The HMEM scheme is based on a hybrid moisture element (HME), whose properties are determined by equivalent moisture capacitance and conductance matrixes calculated using the conventional finite element formulation. A coupled HME-FE scheme is developed and implemented using the commercial FEM software *ABAQUS*. The HME-FE scheme is then employed to analyze the moisture diffusion characteristics of a heterogeneous epoxy resin layer containing particle inclusions. The analysis commences by comparing the performance of the proposed scheme with that of the conventional FEM in modeling the moisture diffusion process. Having validated its performance, the scheme is then employed to investigate the relationship between the volume fraction of the particles in the resin composite and the rate of moisture diffusion. It is found that moisture diffusion is retarded significantly as the volume fraction of particles increases.

The HMEM approach proposed in this study provides a straightforward and efficient means of modeling moisture diffusion in a heterogeneous epoxy resin containing multiple randomly distributed particles since only one HME moisture characteristic matrixes needs to be calculated for all HMEs sharing the same characteristics. Furthermore, different volume fractions can be modeled without modifying the original model simply by controlling the size of the inter-phase region within

[1] Department of Mechanical Engineering, National Chung Cheng University, 168, University Rd., Min-Hsiung, Chia-Yi, 621, Taiwan, R.O.C.

[2] Corresponding author. Tel.: +886-5-2720411 (Ext: 23347); fax: +886-5-2720589 E-mail address: zhenwei@alumni.ccu.edu.tw

[3] Department of Materials Science and Engineering, I-Shou University, No. 1, section 1, Shiuecheng Road, Dashu Shiang, Kaohsiung Country, Taiwan, 840, R.O.C.

[4] RiTdisplay Corporation, No. 12, Kuanfu N. Road, Hsin Chu Industrial Park, 303, Taiwan, R.O.C.

the HME domain.

Keywords: Modeling multiple particles, Heterogeneous epoxy resin, Transient moisture diffusion, Hybrid moisture element method.

1 Introduction

Epoxy resins are widely used in the electronics and optical fields for various applications, including bonding, protecting and encapsulating. In some applications, such as the optical display structure shown in Fig. 1, the epoxy resin is used not only to bond the substrates together, but also to protect the components against disturbances from the external environmental conditions, particularly moisture and oxygen. Therefore, particle fillers are commonly dispersed in the epoxy resin to adjust the material properties and to retard the penetration of moisture into the structure.

The moisture diffusion characteristics of composite materials containing particle fillers have attracted considerable attention [Shen and Springer (1977); Browning, Husman and Whitney (1977)]. Typically, transient moisture diffusion under normal environmental conditions is approximated as a Fickian process and the analytical models designed to explore the moisture diffusion characteristics are based on a homogenized model. In homogeneous materials, the transport of moisture is governed by the maximum moisture content (which generally varies as a strong function of the relative humidity) and by the effective diffusivity (which typically varies as a strong function of the temperature and the volume fraction of the particle fillers). However, the effective or average properties ignore the micro-structural heterogeneity, and hence the homogenized rule-of-mixtures approach may not effectively describe the time variation of the moisture content under transient conditions [Vaddadi, Nakamura and Singh (2003)].

Although analytical methods provide a rapid means of obtaining the effective properties of a matrix-inclusion composite material, such methods can not truly reflect the effect of the randomly distributed particle fillers in the matrix. Therefore, an alternative modeling approach is required. The conventional finite element method (FEM) is commonly employed in such situations since it provides a convenient means of understanding the mechanical behaviors of particle-reinforced composites [e.g., Aditya and Sinha (1996); Vaddadi, Nakamura and Singh (2003); Pahr and Böhm (2008); Takashima, Nakagaki and Miyazaki (2007)]. However, a large number of fine finite elements are required, and mesh modeling is generally a tedious and complicated task, particularly when the aim is to clarify the relationship between the volume fraction of the particles and the specific property of material.

In a series of related studies, Liu and Chiou (2003-2005) discussed the recent de-

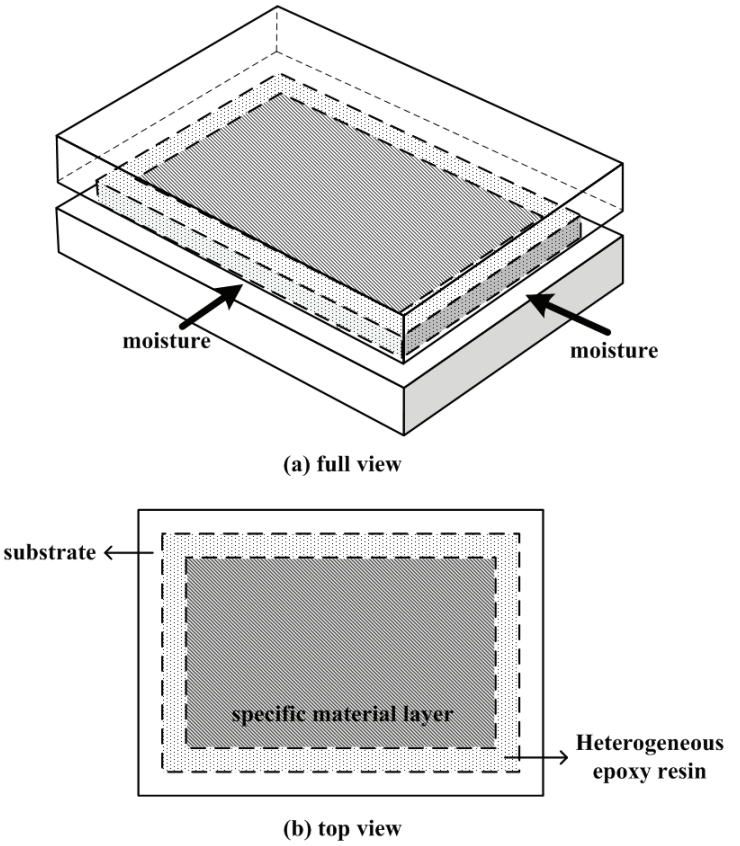

Figure 1: Schematic of optical display structure (not to scale): (a) full view and (b) top view

velopments in 2-D and 3-D infinite element methods (IEM). The conventional IEM approach has been implemented in computer codes to deal with various types of classical elasticity and singularity problems. Liu, Chiou and Chen (2004-2005) also extended the IEM to deal with elastostatic problems in which the constituent material properties are heterogeneous. The related background and knowledge of the earlier work are summarized in the literature [Guo (1979); Ying (1995)]. However, to date, IEM analysis has been limited to the solution of solid mechanics problems.

This study develops a novel, efficient and convenient numerical technique, known as the hybrid moisture element method (HMEM), to characterize moisture diffusion in composite materials containing multiple randomly distributed particles. Taking

the heterogeneous epoxy resin used to bond the two substrates of an optical display structure as an illustrative example, the proposed numerical method is employed to study the transient moisture diffusion process, including the time required to reach a fully saturated state and the effect of varying the volume fraction on the rate of moisture diffusion.

2 Hybrid moisture element method

This section derives a hybrid moisture element formulation for modeling the 2-D moisture diffusion problem. The basis of the proposed method is a hybrid moisture element (HME) containing an inclusion. As shown in Fig. 2, the element domain is decomposed into two separate sub-domains, each with different material characteristics. The two domains represent, respectively: (I) the inter-phase sub-domain with boundaries Γ_0 and Γ_1; and (II) the inclusion sub-domain with a boundary Γ_1. Γ_0 and Γ_1 are, respectively, the element's outer boundary with neighboring elements and the inner interface boundary between the inter-phase and the inclusion sub-domains. The derivations below commence by establishing the element matrix equation.

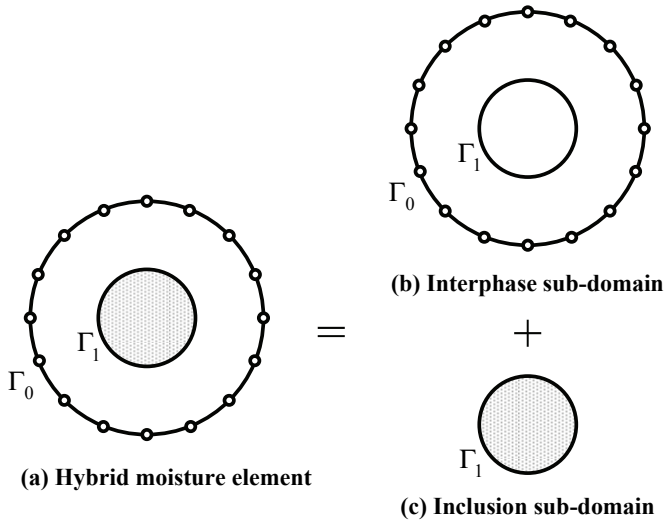

Figure 2: Element decomposition: (a) original hybrid moisture element; (b) inter-phase sub-domain; and (c) inclusion sub-domain

2.1 Governing equation of moisture diffusion

Consider a 2-D plane region with a boundary s. The differential equation for the 2-D moisture diffusion problem is given by

$$\frac{\partial C}{\partial x}\left(D_x\frac{\partial C}{\partial x}\right)+\frac{\partial C}{\partial y}\left(D_y\frac{\partial C}{\partial y}\right)=\frac{\partial C}{\partial t} \tag{1}$$

and has boundary conditions of

$$C=C_0\,|_{s=s_D} \quad \text{and} \quad D_x n_x\frac{\partial C}{\partial x}+D_y n_y\frac{\partial C}{\partial y}=f_B\,|_{s=s_N}\,, \tag{2}$$

where C is the moisture concentration, D_x and D_y are the moisture diffusion coefficients in the x- and y-directions, respectively, n_x and n_y are directional cosines, and f_B is the boundary flux, which has a positive value when directed into the body of interest. Let s_D and s_N respectively denote the parts of s where Dirichlet and Neumann boundary conditions are specified, where $s=s_D\cup s_N$ and $s_D\cap s_N=\emptyset$.

The unit element matrix equation can be obtained from the governing differential equation by applying Galerkin's weighted residual approach. The resulting element matrix equation has the form

$$[M_e]\{\dot{C}_e\}+[K_e]\{C_e\}=\{P_e\}, \tag{3}$$

in which the element moisture capacitance matrix is given by

$$[M_e]=\int [N]^T[N]\,dxdy, \tag{4}$$

the element moisture conductance matrix has the form

$$[K_e]=\int [B]^T[D][B]\,dxdy, \tag{5}$$

and finally

$$\{P_e\}=\int [N]^T f_B\,ds_N. \tag{6}$$

Note that in the equations above, $[B]$ and $[N]$ denote the shape function derivative matrix and the shape function matrix, respectively.

The diffusivity matrix is given by

$$[D]=\begin{bmatrix}D_x & 0\\ 0 & D_y\end{bmatrix}. \tag{7}$$

2.2 2-D hybrid moisture element formulation

In the formulation, the material properties are assumed to be linearly elastic and isotropic, but are heterogeneous from individual sub-domains. The separate formulations for the two sub-domains are derived (index notation is used) as follows:

(I) Formulation in the inter-phase sub-domain:

As shown in Fig. 3(a), the outer boundary of the HME domain, i.e. Γ_0, is properly discretized with a total number of m master nodes (indicated schematically by the symbol "◯"). Taking the global origin O as the similar partition center, and applying a proportionality constant$\lambda \in (0,1)$, a similar polygon, Γ_1, is constructed with the center O, according to the proportionality constant, λ. Straight lines are then drawn from the origin to the master nodes such that Γ_1 is regularly discretized in the same way as Γ_0. The element layer is then auto-meshed into four-node quadrilateral elements in the inter-phase sub-domain.

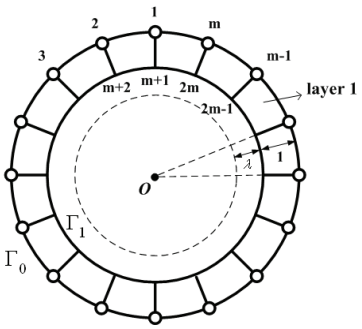

(a) Interphase sub-domain

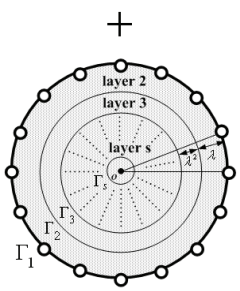

(b) Inclusion sub-domain

Figure 3: Hybrid moisture element mesh: (a) inter-phase sub-domain; and (b) inclusion sub-domain

The element moisture capacitance matrix $[M_e]$ and the element moisture conductance matrix $[K_e]$ of each quadrilateral element in the element layer of the interphase sub-domain (i.e. the region between boundaries Γ_0 and Γ_1) can be calculated and assembled into global matrixes, i.e. $[M]$ and $[K]$, using the conventional finite element formulation. The assembled matrixes of the element layer in the interphase sub-domain are therefore expressed as

$$[M] = \begin{bmatrix} M_a & -B^T \\ -B & M_b \end{bmatrix}_{2\mathrm{m}\times 2\mathrm{m}} \tag{8}$$

and

$$[K] = \begin{bmatrix} K_a & -A^T \\ -A & K_b \end{bmatrix}_{2\mathrm{m}\times 2\mathrm{m}}, \tag{9}$$

where M_a, M_b, and B are sub-matrixes of the assembled matrix $[M]$ with identical dimensions $m \times m$, K_a, K_b, and A are sub-matrixes of the assembled matrix $[K]$ with identical dimensions $m \times m$, and B^T and A^T are the transposes of B and A, respectively. Since the element layer matrixes $[M]$ and $[K]$ are globally symmetrical and banded, matrixesM_a, M_b, K_a, and K_b are also symmetrical and banded.

The nodal moisture concentration vector C_i of the nodes on Γ_i is defined as

$$C_i \equiv \begin{bmatrix} C_1^i & C_2^i & \cdots & C_m^i \end{bmatrix}^T, \tag{10}$$

and

$$\dot{C}_i \equiv \begin{bmatrix} \dot{C}_1^i & \dot{C}_2^i & \cdots & \dot{C}_m^i \end{bmatrix}^T. \tag{11}$$

The nodal loading vector P_i of the nodes on Γ_i is defined as

$$P_i \equiv \begin{bmatrix} P_1^i & P_2^i & \cdots & P_m^i \end{bmatrix}^T. \tag{12}$$

Therefore, the element matrix equation can be expressed as

$$\begin{bmatrix} M_a & -B^T \\ -B & M_b \end{bmatrix} \cdot \begin{bmatrix} \dot{C}_0 \\ \dot{C}_1 \end{bmatrix} + \begin{bmatrix} K_a & -A^T \\ -A & K_b \end{bmatrix} \cdot \begin{bmatrix} C_0 \\ C_1 \end{bmatrix} = \begin{bmatrix} P_0 \\ P_1 \end{bmatrix}. \tag{13}$$

Two algebraic equations can then be extracted from Eq. (13), i.e.

$$M_a \cdot \dot{C}_0 - B^T \cdot \dot{C}_1 + K_a \cdot C_0 - A^T \cdot C_1 = P_0 \tag{14}$$

and

$$-B \cdot \dot{C}_0 + M_b \cdot \dot{C}_1 - A \cdot C_0 + K_b \cdot C_1 = P_1. \tag{15}$$

(II) Formulation in the inclusion sub-domain:

The partition processes for the inclusion sub-domain as shown in Fig. 3(b) are similar to processes for the inter-phase sub-domain. The inner boundary Γ_1 of the inter-phase region is exactly the outer boundary of the inclusion region. Also, when the global origin O is chosen as the similar partition center and when proportionality constant λ and element-layers s are taken, similar polygons Γ_2, Γ_3, $\cdots$, Γ_s of Γ_0 are generated with center O according to the proportionality constants λ^2, λ^3, $\cdots$, λ^s, respectively. The region bounded between Γ_{i-1} and Γ_i is called the *i-th* element-layer (i= 1, 2, 3$\cdots$, s). Straight lines are drawn from the origin to the master nodes, and each individual Γ_i is regularly discretized, like Γ_0. The nodal number and coordinates of nodes on each individual Γ_i can be determined from the master node coordinates with geometrically similar conditions. Every element-layer is auto-meshed into four-node quadrilateral elements that are similar to one another from the element-layers in a radial direction. The assembled matrixes of the outermost element-layer (*2nd* element-layer) in the inclusion sub-domain can be calculated and expressed as

$$[M_\Delta] = \begin{bmatrix} M_{\Delta a} & -B_\Delta^T \\ -B_\Delta & M_{\Delta b} \end{bmatrix}_{2\mathrm{m}\times 2\mathrm{m}} \tag{16}$$

and

$$[K_\Delta] = \begin{bmatrix} K_{\Delta a} & -A_\Delta^T \\ -A_\Delta & K_{\Delta b} \end{bmatrix}_{2\mathrm{m}\times 2\mathrm{m}}. \tag{17}$$

According to the similarity principle, it is obvious that the element moisture capacitance matrixes of all of the element-layers are in dimensional dependence on the ratio λ^2 and the element moisture conductance matrixes of all of the element-layers are identical. Hence, we can express the element matrix of the s-1 element-layers (from the *2nd* element-layer to the *s-th* element-layer) as a set of algebraic equations, namely

$$\begin{bmatrix} M_{\Delta a} & -B_\Delta^T \\ -B_\Delta & M_{\Delta b} \end{bmatrix} \cdot \begin{bmatrix} \dot{C}_1 \\ \dot{C}_2 \end{bmatrix} + \begin{bmatrix} K_{\Delta a} & -A_\Delta^T \\ -A_\Delta & K_{\Delta b} \end{bmatrix} \cdot \begin{bmatrix} C_1 \\ C_2 \end{bmatrix} = \begin{bmatrix} -P_1 \\ P_2 \end{bmatrix} \tag{18}$$

for layer 2.

$$\lambda^2 \cdot \begin{bmatrix} M_{\Delta a} & -B_\Delta^T \\ -B_\Delta & M_{\Delta b} \end{bmatrix} \cdot \begin{bmatrix} \dot{C}_2 \\ \dot{C}_3 \end{bmatrix} + \begin{bmatrix} K_{\Delta a} & -A_\Delta^T \\ -A_\Delta & K_{\Delta b} \end{bmatrix} \cdot \begin{bmatrix} C_2 \\ C_3 \end{bmatrix} = \begin{bmatrix} -P_2 \\ P_3 \end{bmatrix} \tag{19}$$

for layer 3.

$$\lambda^4 \cdot \begin{bmatrix} M_{\Delta a} & -B_\Delta^T \\ -B_\Delta & M_{\Delta b} \end{bmatrix} \cdot \begin{bmatrix} \dot{C}_3 \\ \dot{C}_4 \end{bmatrix} + \begin{bmatrix} K_{\Delta a} & -A_\Delta^T \\ -A_\Delta & K_{\Delta b} \end{bmatrix} \cdot \begin{bmatrix} C_3 \\ C_4 \end{bmatrix} = \begin{bmatrix} -P_3 \\ P_4 \end{bmatrix} \tag{20}$$

for layer 4.

$$\vdots$$

$$\lambda^{2(s-1)} \cdot \begin{bmatrix} M_{\Delta a} & -B_{\Delta}^{T} \\ -B_{\Delta} & M_{\Delta b} \end{bmatrix} \cdot \begin{bmatrix} \dot{C}_{s-1} \\ \dot{C}_{s} \end{bmatrix} + \begin{bmatrix} K_{\Delta a} & -A_{\Delta}^{T} \\ -A_{\Delta} & K_{\Delta b} \end{bmatrix} \cdot \begin{bmatrix} C_{s-1} \\ C_{s} \end{bmatrix} = \begin{bmatrix} -P_{s-1} \\ P_{s} \end{bmatrix} \tag{21}$$

for layer s.

In modeling the inclusion sub-domain of the HME, an assumption is made that the inclusion can absorb only a small amount of moisture and proportionality constants λ is always less than one. Therefore, the diffusivity terms in Eq. (18-21) could be approximated as negligible. Extracting with every algebraic equation, combining the second equation for the *i-th* element-layer and the first equation for the *(i+1)-th* element-layer and letting $Q = K_{\Delta a} + K_{\Delta b}$, we have

$$K_{\Delta a} \cdot C_1 - A_{\Delta}^{T} \cdot C_2 = -P_1 \tag{22}$$

$$-A_{\Delta} \cdot C_1 + Q \cdot C_2 - A_{\Delta}^{T} \cdot C_3 = 0 \tag{23}$$

$$\vdots$$

$$-A_{\Delta} \cdot C_{i-1} + Q \cdot C_i - A_{\Delta}^{T} \cdot C_{i+1} = 0 \tag{24}$$

$$\vdots$$

$$-A_{\Delta} \cdot C_{s-2} + Q \cdot C_{s-1} - A_{\Delta}^{T} \cdot C_s = 0 \tag{25}$$

$$-A_{\Delta} \cdot C_{s-1} + K_{\Delta b} \cdot C_s = P_s \equiv F_s \tag{26}$$

Let $M_s = K_{\Delta b}$ and $F_s \equiv P_s$ and substitute them into Eq. (26), we have

$$C_s = M_s^{-1} \cdot (A_{\Delta} \cdot C_{s-1} + F_s) \tag{27}$$

By substituting Eq. (27) into Eq. (25), we get

$$-A_{\Delta} \cdot C_{s-2} + \left(Q - A_{\Delta}^{T} \cdot M_s^{-1} \cdot A_{\Delta}\right) \cdot C_{s-1} = A_{\Delta}^{T} \cdot M_s^{-1} \cdot F_s \tag{28}$$

When Eq. (28) is compared with Eq. (27), two iteration formulas can be inferred as follows:

$$M_k = Q - A_{\Delta}^{T} \cdot M_{k+1}^{-1} \cdot A_{\Delta} \tag{29}$$

$$F_k = A_{\Delta}^{T} \cdot M_{k+1}^{-1} \cdot F_{k+1} \tag{30}$$

where k= 2, 3, 4…, s-1.

By substituting the above two iteration formulas into Eq. (28), we get

$$-A_\Delta \cdot C_{s-2} + M_{s-1} \cdot C_{s-1} = F_{s-1} \tag{31}$$

When Eq. (31) is rearranged, another iteration formula can be inferred, as follows:

$$C_l = M_l^{-1} \cdot (A_\Delta \cdot C_{l-1} + F_l) \tag{32}$$

where l= 2, 3, 4…, s.

From Eq. (32), we have

$$C_2 = M_2^{-1} \cdot (A_\Delta \cdot C_1 + F_2) \tag{33}$$

By substituting Eq. (33) into Eq. (22), we get

$$K_{\Delta a} \cdot C_1 - A_\Delta^T \cdot \left[M_2^{-1} \cdot (A_\Delta \cdot C_1 + F_2)\right] = -P_1 \tag{34}$$

Rearranging Eq. (34), we have

$$\left(K_{\Delta a} - A_\Delta^T \cdot M_2^{-1} \cdot A_\Delta\right) \cdot C_1 = \left[A_\Delta^T \cdot M_2^{-1} \cdot F_2 + (-P_1)\right] \tag{35}$$

Eq. (35) can be expressed in the concise form

$$K_{(inclusion)} \cdot C_1 = F_{(inclusion)} \tag{36}$$

where $K_{(inclusion)}$ and $F_{(inclusion)}$ denote the equivalent moisture conductance matrix and associated loading vector for the inclusion sub-domain, respectively. Along the inclusion/inter-phase interface Γ_1, however, the moisture compatibility and force equilibrium must be satisfied. Therefore, Eq. (15) and (35) are combined and we have

$$-B \cdot \dot{C}_0 - A \cdot C_0 + \left(K_b + K_{\Delta a} - A_\Delta^T \cdot M_2^{-1} \cdot A_\Delta\right) \cdot C_1 = A_\Delta^T \cdot M_2^{-1} \cdot F_2. \tag{37}$$

Let $K_{b(modified)} = K_b + K_{\Delta a} - A_\Delta^T M_2^{-1} A_\Delta$ and substitute it into Eq. (37), we have

$$C_1 = K_{b(modified)}^{-1} \cdot B \cdot \dot{C}_0 + K_{b(modified)}^{-1} \cdot A \cdot C_0 + K_{b(modified)}^{-1} \cdot A_\Delta^T \cdot M_2^{-1} \cdot F_2. \tag{38}$$

Since M_s and F_s are known, then M_{s-1}, M_{s-2}, $\cdots$, M_2; F_{s-1}, F_{s-2}, $\cdots$, F_2 can be iterated out using equations (29) and (30), respectively. From Eq. (38), Substituting C_1 into Eq. (14), we obtain the most important equation, that is,

$$\begin{aligned} &\left(M_a - A^T \cdot K_{b(modified)}^{-1} \cdot B\right) \cdot \dot{C}_0 + \left(K_a - A^T \cdot K_{b(modified)}^{-1} \cdot A\right) \cdot C_0 \\ &= P_0 + A^T \cdot K_{b(modified)}^{-1} \cdot A_\Delta^T \cdot M_2^{-1} \cdot F_2 \end{aligned} \tag{39}$$

Eq. (39) can be expressed in concise form as:

$$M_Z \cdot \dot{C}_0 + K_Z \cdot C_0 = F_Z \tag{40}$$

where $M_Z = \left(M_a - A^T \cdot K^{-1}_{b(modified)} \cdot B\right)$ and $K_Z = \left(K_a - A^T \cdot K^{-1}_{b(modified)} \cdot A\right)$ are the combined element moisture capacitance and conductance matrixes, respectively. $F_Z = \left(P_0 + A^T \cdot K^{-1}_{b(modified)} \cdot A^T_\Delta \cdot M_2^{-1} \cdot F_2\right)$ is the associated loading vector. In other words, M_Z and K_Z can be regarded as the equivalent moisture capacitance and conductance matrixes of the hybrid moisture element. Once C_0 is solved, C_1 can be obtained from Eq. (38). Then C_2, C_3, $\cdots$, and C_s can be obtained sequentially from Eq. (32).

In the current analysis, it is assumed that the boundary flux is zero and that only the Dirichlet boundary condition is applied, i.e. only concentrations are prescribed at the boundaries. Therefore, the element matrix equation can be rewritten as:

$$M_Z \cdot \dot{C}_0 + K_Z \cdot C_0 = 0 \tag{41}$$

2.3 Implementation of coupled HME-FE scheme using commercial FEM software

In the proposed coupled HME-FE scheme, the HME is used to replace specific parts of the entire FE domain. It implies the particle inclusions in the FE domain are all replaced by HMEs. Fig. 4 shows a schematic representation of the coupled scheme. As shown, the global model is partitioned into two separate domains, namely Ω and D, modeled using the HME and FE, respectively.

The related HMEM numerical procedures were programmed and executed in the MATLAB language [Kwon and Bang (2000)]. Following the HMEM mathematical manipulations, the HME was generated (see Section 2.2). The HME can be regarded as a regular finite element, whose properties are derived from the predetermined HME moisture capacitance and conductance matrixes, M_Z and K_Z. In this study, the HME-FE coupled scheme was executed using the commercial FEM software, ABAQUS. However, the HME definition is not included in the ABAQUS element library. Therefore, the HME is designated as a user-defined element that represents a geometric part of the model.

In the ABAQUS codes, the user-defined elements are introduced using the *USER ELEMENT option. In general cases, a linear user-defined element can be represented as moisture capacitance and conductance matrixes, which can be distilled from the MATLAB results (M_Z and K_Z, respectively) and defined using the *MATRIX option. The numerical property values associated with these linear user-defined elements are defined using the *UEL PROPERTY option and, optionally,

the *MATRIX option. Further details of this implementation are presented in the ABAQUS user manual [Hibbitt, Karlsson and Sorensen (2004)].

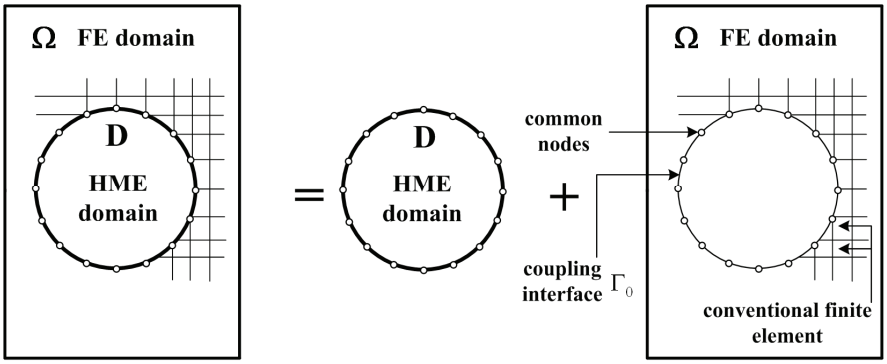

Figure 4: Schematic diagram of coupled HME-FE scheme

2.4 Mesh modeling technique of random HME inclusions

The epoxy resin with the random-particles arrangement was generated using the uniform random number generator in MATLAB language [Kwon and Bang (2000)]. Each coordinate was produced independently, with another random number seed. After the coordinates of a first particle were defined, the coordinates of each new particle were determined both by using the random number generator, and from the condition that the distance between the new particle and all available particles is no less than 0.1 of the given particle radius. If the condition was not met, the seed of the random number generator was changed, and the coordinates of the new particle were determined anew. In order to avoid mesh distortion and improper elements, the distance between a particle and borders of the box was required to be no less than 0.1 particle radius.

To apply multiple randomly dispersed inclusions, the mesh modeling technique of the randomly distributed HME-domain inclusions conducted in this study was performed using self-written codes by ANSYS Parametric Design Language (APDL). To exploit HME-FE coupling method, the shape and region of inclusions should first be considered and reserved in the mesh modeling process, as shown in Fig. 5. Moreover, all the master nodes for each HME must keep the same nodal sequence to ensure that their assembled matrixes remain the same. Therefore, modeling composite material reinforced with multiple randomly distributed inclusions involves calculating only one HME moisture characteristic matrixes, using particular finite element mesh modeling. In this study, APDL is employed to construct

master nodes on the surface of each inclusion with the same nodal permutation related with corresponding partition center, and the master nodes are then merged into the FE model. Hence, engineering problems with complicated geometric shape can be modeled more conveniently.

As shown in Fig. 5, the HME domain of the HME-FE computational model comprises the particles (i.e. the inclusion regions) and the surrounding material (i.e. the inter-phase regions). The material properties in the inter-phase region are identical to those in the epoxy matrix region, and hence the inter-phase regions are not explicitly modeled. Furthermore, it is assumed that a perfect bonding exists between the particles and the matrix. Therefore, different particle volume fractions can be modeled without modifying the original model simply by controlling the size of the inter-phase region within the HME domain. Additionally, it is only necessary to calculate a single HME moisture capacitance and conductance matrixes for all HMEs with the same characteristics. After mesh modeling has been completed, ABAQUS is utilized to integrate HME and conventional FE in the solution process.

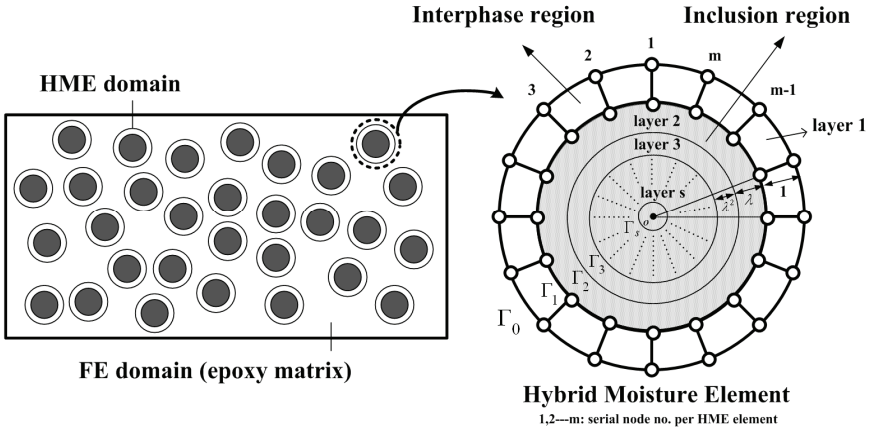

Figure 5: Epoxy resin with multiple randomly arranged particles used in HME-FE computational model

HMEM can automatically generate a series of layer-wise virtual element with similar shapes according to the center of the similarity and proportionality constant within the reserved region, and thus only needs to construct the element for the FE region in the HME-FE mesh modeling process. Therefore, the HME-FE coupling method significantly reduces the execution time in the mesh modeling stage, the number of degrees of freedom (DOFs) and the PC memory storage requirement.

3 Moisture diffusion modeling

In the current modeling method, the transient moisture diffusion equation is analogous to that of heat conduction. The analogous technique for a homogeneous material system [Crank and Park (1956)] has recently been extended to a multi-material system [Wong, Teo and Lim (1998); Wong, Rajoo, Koh and Lim (2002)], and hence it is suitable for the current analysis of moisture diffusion in a heterogeneous epoxy resin filled with particles.

To enable the moisture diffusion problem to be treated as a typical heat transfer problem using commercial finite element analysis software, a moisture wetness variable, W, is introduced, and is defined as

$$\mathrm{W} = \frac{C}{C_{\mathrm{sat}}}, \quad 1 \geq \mathrm{W} \geq 0, \tag{42}$$

where C_{sat} is the maximum moisture concentration that can be absorbed by the material. The lower limit of W, i.e. $\mathrm{W} = 0$, indicates that the material is completely dry, while the upper limit, i.e. $\mathrm{W} = 1$, indicates that the material is fully saturated with moisture. The "wetness" thermal-moisture analogy scheme for the current finite element implementation is presented in Tab. 1.

Table 1: FEA thermal-moisture analogy for moisture diffusion modeling

Properties	Thermal	Moisture
Field variable	Temperature, T	Wetness, W
Density	ρ(kg / m^3)	1
Conductivity	K(W / m $\cdot$ °C)	$D * C_{\mathrm{sat}}$(kg / s $\cdot$ m)
Specific capacity	c(J / kg $\cdot$ °C)	C_{sat}(kg / m^3)

4 Validation of HME-FE model

This section presents two examples to validate the performance of the proposed HME-FE modeling approach.

Fig. 6 (right panel) shows the HME-FE computational model with 3 inclusions and with length and width dimensions (i.e. the length to width ratio is 4:3). In this figure, D represents the HME sub-domain and Ω represents the FE sub-domain. As shown, the inclusions are circular, and have a radius 7.5 times smaller than the model length. A moisture condition of 85°C/85% RH is applied at the left edge and hence the moisture permeates from the exposed surface on the left of the model and diffuses toward the right. The moisture related material properties,

i.e. the diffusivity and C_{sat}, characterized under the applied moisture conditions of 85°C/85% RH, are 54.4×10^{-14}m^2 / s and 16mg / cm^3, respectively.

The right panels of Fig. 6-8 show the HME-FE modeling results for the moisture profiles at three different time steps. The HMEM parameters are: $\lambda = 0.9$ and $s = 100$. In the HME-FE model, a total of 96 master nodes are used, with 32 nodes on each of the 3 HME sub-domain, and 826 four-node quadrilateral elements in the FE sub-domain. The corresponding results obtained from the conventional FEM scheme are presented in the left panels for comparison purposes. In the conventional FE model, the total number of elements was 922 and the total number of nodes was 1038. Tab. 2 shows the comparisons of both methods by execution time and number of DOFs on an AMD Dual-Core-2.21 GHz computer at the 60^{th} time step. Comparing the two sets of transient moisture distributions, it is apparent that the HME-FE results differ slightly from the FEM results, but the basic trends of the two sets of transient moisture distributions are very similar. The little discrepancy between HME-FE and FEM is due to the conventional FE model used voids replacing particles to avoid complicated meshing process [Vaddadi, Nakamura and Singh (2003); Laureenzi, Albrizio and Marchetti (2008)]; therefore, the equivalent DOFs in the HME-FE model are much greater than those in the conventional FE model.

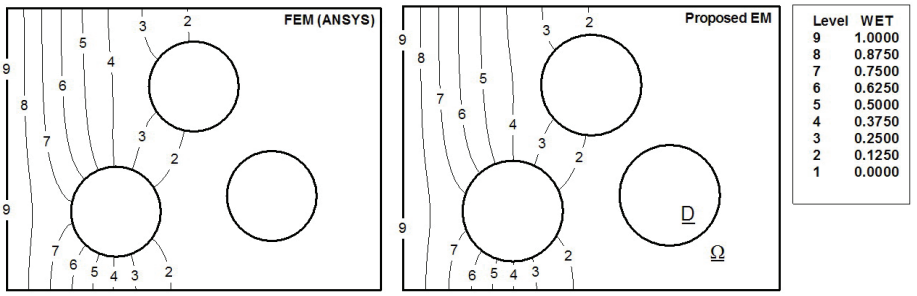

Figure 6: Moisture distribution at the 8^{th} time step for moisture conditions of 85°C/85% RH

Table 2: Execution time and DOFs of the HME-FE and FEM approaches

Numerical method	Execution time (s)	Total nodes	Total DOFs	Equivalent DOFs
HME-FE	0.7	942	942	4142
FEM (ANSYS)	1.53	1038	1038	1038

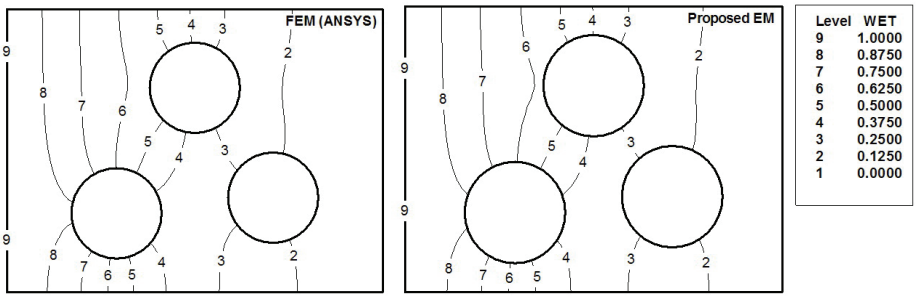

Figure 7: Moisture distribution at the 24^{th} time step for moisture conditions of 85°C/85% RH

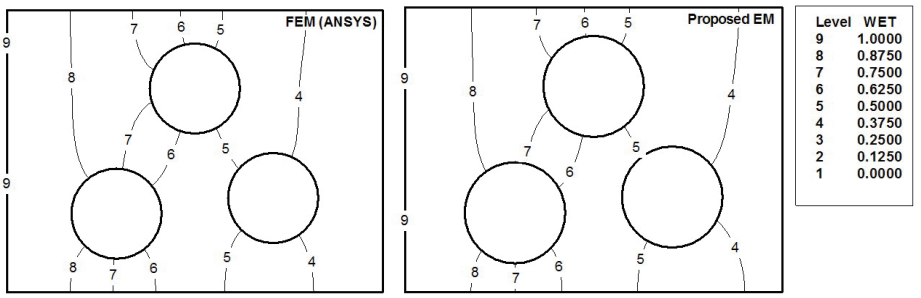

Figure 8: Moisture distribution at the 60^{th} time step for moisture conditions of 85°C/85% RH

In the second validation example, Fig. 9 plots the variation of the level of wetness of the epoxy resin after various time steps in an HME-FE computational model with a length to thickness ratio of 5:1 and a 45% volume fraction of particles. The HMEM parameters are: $\lambda = 0.9708$ and $s = 100$. In the HME-FE model, a total of 912 master nodes are used, with 12 nodes on each of the 76 HME sub-domain, and 1105 four-node quadrilateral elements in the FE sub-domain. In the conventional FE model, the total number of elements was 1107 and the total number of nodes was 1585. Tab. 3 shows the comparisons of both methods by execution time and number of DOFs on an AMD Dual-Core-2.21 GHz computer at the 250^{th} time step. It can be seen that the results obtained from the HME method are in good general agreement with those obtained from the FEM approach. However, it is observed that the HMEM scheme estimates a slightly shorter time required to achieve a fully saturated state than the FEM model.

As described previously, the proposed HMEM provides a straightforward and efficient means of modeling moisture diffusion in epoxy resin filled with particles since only one HME moisture capacitance and conductance matrixes needs to be calculated for all HMEs with the same properties. Furthermore, all of the DOFs related to the HME domain are condensed and transformed to form a combined element with master node DOFs only. Therefore, the total number of DOFs and the PC memory storage requirements are reduced. Most importantly, different particle volume fractions can be modeled without modifying the original model simply by controlling the size of the inter-phase region within the HME domain. This advantage of the HME approach becomes particularly apparent when the scheme is applied to investigate the relationship between the particle volume fraction and the moisture diffusion characteristics of a heterogeneous material filled with multiple particles.

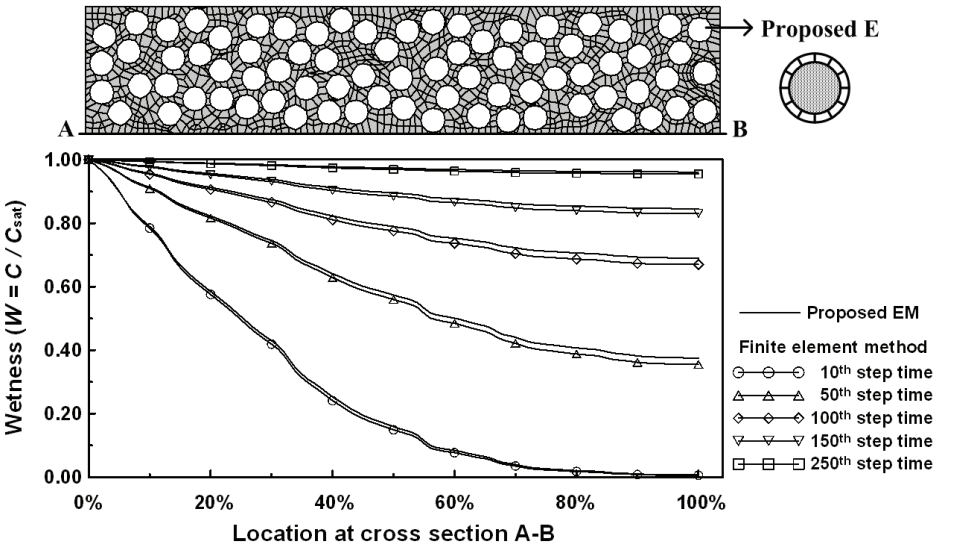

Figure 9: Moisture diffusion from 10^{th} to 250^{th} time step

5 Moisture diffusion in heterogeneous epoxy resin containing multiple randomly distributed particles

In examining the moisture diffusion properties of a heterogeneous material containing various volume fractions of particles, the present analysis considers the case of the epoxy resin used to bond the substrates of an optical display structure, e.g. an

Table 3: Execution time and DOFs of the HME-FE and FEM approaches

Numerical method	Execution time (s)	Total nodes	Total DOFs	Equivalent DOFs
HME-FE	7.3	1571	1571	92771
FEM (ABAQUS)	13.2	1585	1585	1585

organic light emitting display (OLED) or a liquid crystal display (LCD). In general, the epoxy resin not only bonds the two substrates together, but also protects the inner components against disturbances from the external environment. The inner specific material layer of these optical displays is highly sensitive to moisture. Therefore, the particle fillers which are generally added to the epoxy resin are designed not only to adjust the material properties, but also to retard moisture penetration.

The present analysis considers a simple 2-D structure comprising an epoxy resin with multiple randomly distributed particles, as shown in Fig. 10. The epoxy resin is assumed to be heterogeneous and to have a length and width of 500μm and 50μm, respectively (i.e. a thickness ratio of 10:1). A moisture condition of 85°C/85% RH is applied at the left side of the structure. The moisture related properties of the epoxy resin are presented in Tab. 4.

Table 4: Material properties

Property	Particles	Epoxy resin
Moisture diffusivity (85°C/85% RH)	0	54.4×10^{-14} m^2 / s
Saturated moisture concentration (85°C/85% RH)	0	16 mg / cm^3

5.1 Transient moisture diffusion process

The transient moisture diffusion process in the 2-D composite material with multiple randomly distributed particles (inclusions) shown in Fig. 10 was analyzed using the proposed HME-FE computational model. To represent a typical heterogeneous epoxy resin, the modeling considered a random inclusion configuration with a particle volume fraction of 45% (vf =0.45). The particles were assumed to be circular with a radius of r=2.5μm, i.e. the particle radius was 20 times smaller than the thickness of the epoxy resin structure. The inclusions were prevented from over-

lapping in the random inclusion configuration by specifying a minimum separation distance of 0.1r. Finally, the surface was exposed to a humidity of 85% RH. As described previously, in the computational model, the regions of the epoxy resin occupied by the particles were replaced by HMEs such that only one HME moisture capacitance and conductance matrixes needs to be calculated for all of the same HMEs. Hence, the total number of DOFs and the PC memory storage requirements are reduced. The HMEM parameters are: $\lambda = 0.9772$ and $s = 100$. In the HME-FE model, a total of 7200 master nodes are used, with 12 nodes on each of the 600 HME sub-domain, and 7946 four-node quadrilateral elements in the FE sub-domain.

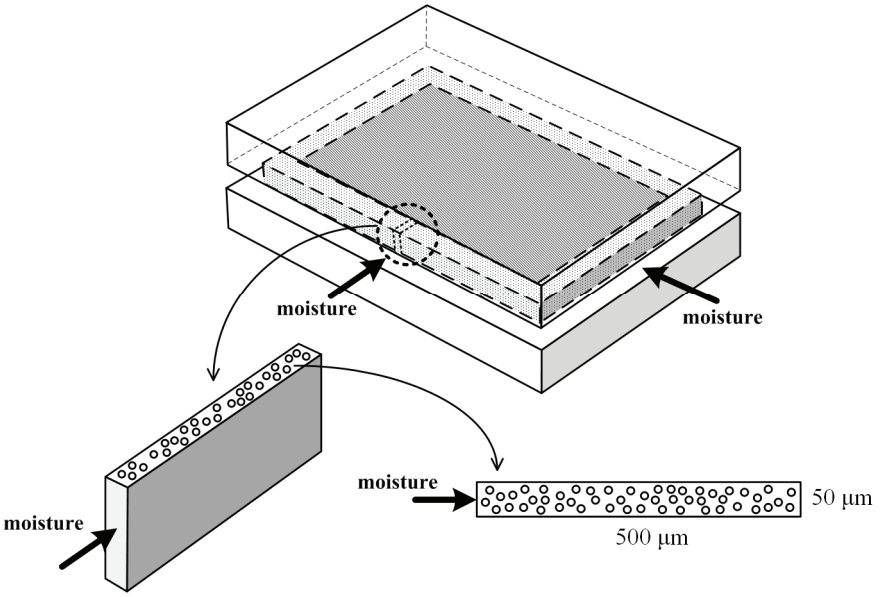

Figure 10: Simplified 2-D structure comprising heterogeneous epoxy resin bonding layer and substrates

Using a gray-scale notation, Fig. 11 illustrates the moisture distribution profiles within the composite epoxy structure at four different moisture exposure times, i.e. 10, 50, 100 and 150 hrs, respectively. In the region close to the exposed surface, it is apparent that the moisture content immediately becomes saturated, i.e. the moisture wetness variable attains a value of W = 1. In fact, this represents the boundary condition prescribed along the exposed plane. The moisture is then transported progressively along the epoxy resin structure as the moisture exposure time increases.

Fig. 12 illustrates the variation of the moisture wetness of the epoxy resin structure adjacent to the lower boundary with the elapsed exposure time. After 200 hours, the variation of the moisture wetness along the length of the epoxy resin structure is very small, i.e. the entire epoxy resin is almost fully saturated with moisture. Since the composite material can only absorb a finite amount of moisture, the moisture content increases only slightly as the exposure time is further increased to 250 hrs.

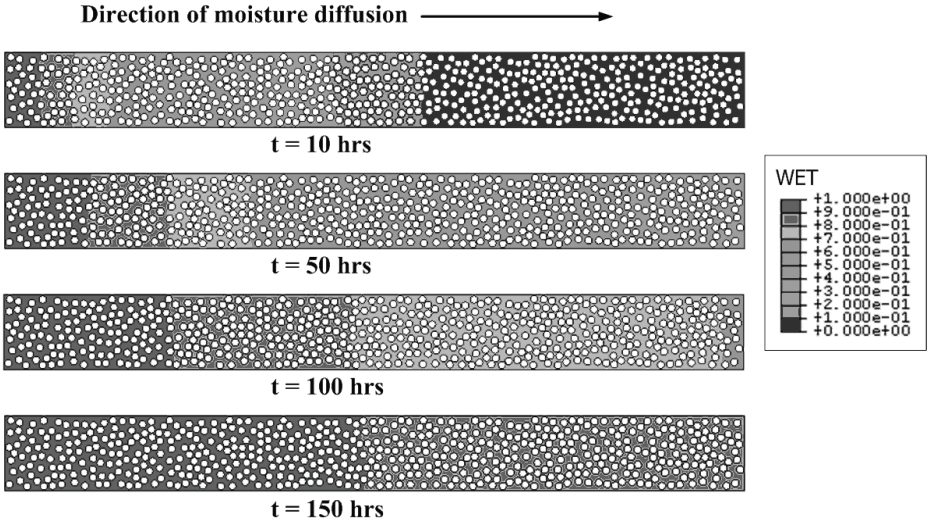

Figure 11: Transient moisture distribution at different moisture exposure times

5.2 Influence of volume fraction of particles on moisture diffusion

The HME-FE scheme was applied to investigate the moisture diffusion characteristics of epoxy resins containing randomly distributed particles with various volume fractions, i.e. five to 45 percent in nine equal steps, respectively. The corresponding results are presented in Fig. 13 and 14.

In the HME sub-domain of the HME-FE computational model, the material properties in the inter-phase region are identical to those in the matrix region (i.e. the epoxy matrix). Therefore, the inter-phase is not modeled explicitly. Furthermore, it is assumed that a perfect bonding exists between the particles and the matrix. Hence, different particle volume fractions can be modeled without modifying the original model simply by controlling the size of the inter-phase region within the HME domain. Tab. 5 lists the HMEM parameters about the proportionality constants λ and the numbers of element-layers s for each studied volume fraction. In

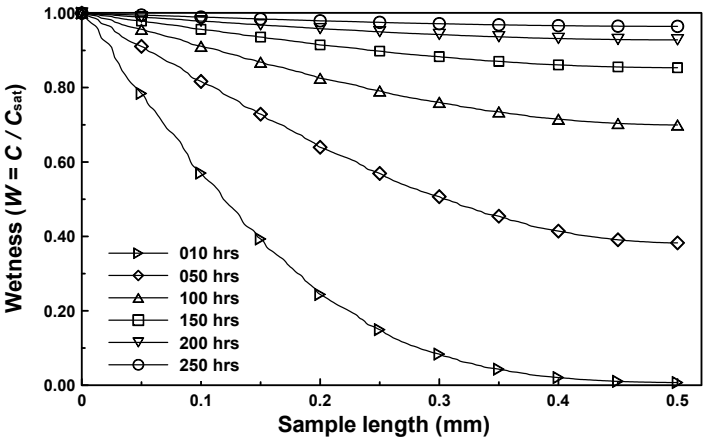

Figure 12: Moisture diffusion in epoxy resin with vf=0.45 from 10 to 250 hrs

the random particle HME-FE model, a total of 7200 master nodes are used, with 12 nodes on each of the 600 HME sub-domain, and 7946 four-node quadrilateral elements in the FE sub-domain.

Table 5: HMEM parameters for each studied volume fraction

Volume fraction	λ	s
5%	0.3257350079	100
10%	0.4606588659	100
15%	0.564189583	100
20%	0.6514700158	100
25%	0.7283656203	100
30%	0.7978845608	100
35%	0.8618138243	100
40%	0.9213177319	100
45%	0.9772050238	100

Fig. 13 shows the effect of varying volume fraction of particles, i.e. 30 to 45 percent in four steps, in epoxy resin on moisture diffusion. The moisture which reaches the far end of the epoxy structure reduces as the volume fraction of the particles increases. The physical explanation for this is that the randomly distributed particles impede moisture transfer, particularly at higher volume fractions.

Moreover, as shown in Fig. 14, the time taken to attain a fully saturated state (i.e.

the variation of the moisture wetness in the epoxy resin is less than 1%) depends on the particle volume fraction. Specifically, the time required to reach the moisture saturation condition increases with an increasing volume fraction of particles. From inspection, it is found that the time required to reach saturation conditions in the epoxy resin containing randomly distributed particles with a volume fraction of 45% is more than twice that in the resin with a volume fraction of 5% . Therefore, it is clear that the volume fraction of the particles has a notable influence on the time required for a heterogeneous composite to reach a fully saturated state.

The results of Fig. 13 and 14 imply that an optical display structure should be constructed using a bonding epoxy resin containing a high volume fraction of particles in order to provide the inner components with maximum protection against the effects of moisture penetration.

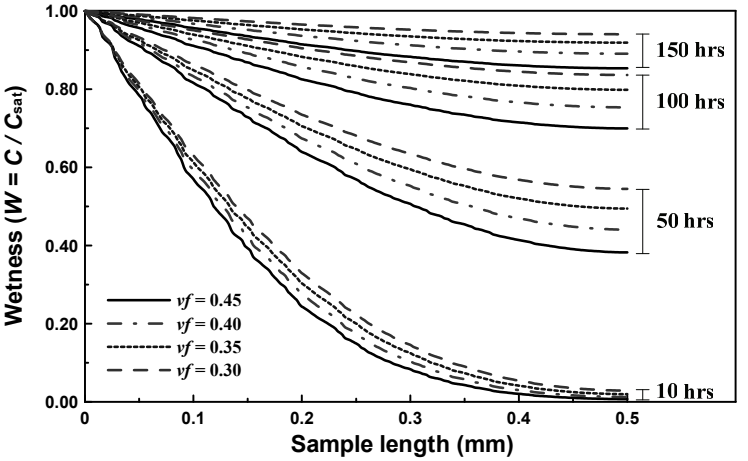

Figure 13: Effect of varying volume fraction of particles in epoxy resin on moisture diffusion

6 Conclusion

This study has developed a hybrid moisture element method (HMEM) for modeling and analyzing moisture diffusion in a heterogeneous epoxy resin containing multiple randomly distributed particles. The HMEM modeling approach is based on hybrid moisture elements (HMEs), whose characteristics are determined by an equivalent moisture capacitance and conductance matrixes calculated using the conventional finite element formulation. A coupled HME-FE scheme has been developed and implemented using the commercial FEM software ABAQUS.

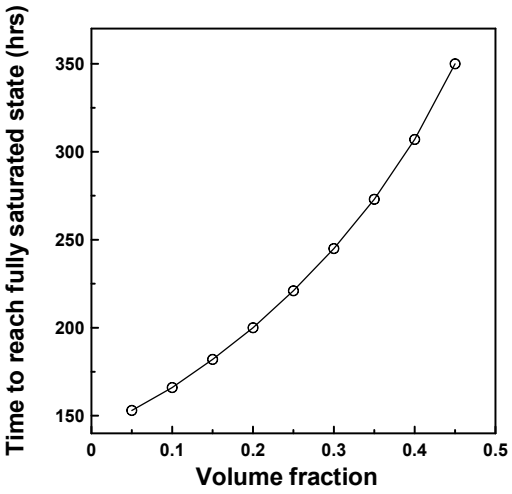

Figure 14: Effect of varying volume fraction of particles in epoxy resin on time required to reach fully saturated state

Having first validated the performance of the proposed HME-FE method by comparing the results obtained for the moisture distribution profiles in a heterogeneous epoxy resin layer with those obtained from the conventional FEM scheme, the modeling approach was employed to investigate various aspects of the transient moisture diffusion process in an optical display structure bonded using a heterogeneous epoxy resin. Specifically, the analysis investigated the effect of the volume fraction of particles on the rate of moisture diffusion and the time required to reach a saturated state. The results showed that the amount of moisture which penetrates into the resin layer reduces significantly as the fraction volume of particles increases. Therefore, it can be inferred that an optical display structure should be constructed using a bonding epoxy resin with a high volume fraction of particles in order to protect the inner components against moisture ingression.

The modeling approach proposed in this study has a number of key advantages when applied to the analysis of moisture diffusion in heterogeneous materials with embedded multiple inclusions. Firstly, in the computational model, the regions of the epoxy resin occupied by the particles are all replaced by HMEs such that only one HME moisture capacitance and conductance matrixes needs to be calculated for all HMEs with the same characteristics. Hence, the total number of DOFs in the computational model and the PC memory storage and processing requirements are significantly reduced. Secondly, different volume fractions of particles can be modeled without modifying the original model simply by controlling the size of

the inter-phase region within the HME domain. Finally, the results obtained from the proposed method are in good general agreement with those of the conventional FEM scheme.

Acknowledgement: The current authors gratefully acknowledge the financial support provided to this study by the National Science Council, Taiwan, R. O. C., under Grant NO. NSC98-2627-E-194-001 and NSC98-2221-E-194-014-MY3.

References

Aditya, P.K.; Sinha, P.K. (1996): Moisture diffusion in variously shaped fibre reinforced composites. *Comput. Struct.*, vol. 59, no. 1, pp. 157-166.

Browning, C.E.; Husman, G.E.; Whitney, J.M. (1977): Moisture effects in epoxy resin matrix composites. *Composite Materials: Testing and Design, ASTM STP 617*, pp. 481-496.

Crank, J.; Park, G.S. (1956): *The Mathematics of Diffusion*. Oxford University Press.

Guo, Z.H. (1979): Similar isoparametric elements. *Sci. Bull.*, vol. 24, no. 13, pp. 577-582.

Hibbitt, D.; Karlsson, B.; Sorensen, P. (2004): *ABAQUS User's Manual Version 6.5*. Pawtucket, RI.

Kwon, Y.W.; Bang, H. (2000): *The Finite Element Method using MATLAB, second ed.* CRC Press, New York.

Laurenzi, S.; Albrizio, T.; Marchetti, M. (2008): Modeling of Moisture Diffusion in Carbon Braided Composites. *International Journal of Aerospace Engineering*, vol. 2008, article id. 294681, 10 pages.

Liu, D.S.; Chiou, D.Y. (2003): A coupled IEM/FEM approach for solving the elastic problems with multiple cracks. *Int. J. Solids Struct.*, vol. 40, pp. 1973-1993.

Liu, D.S.; Chiou, D.Y. (2003): 3D IEM formulation with an IEM/FEM coupling scheme for solving elastostatic problems. *Adv. Eng. Softw.*, vol. 34, pp. 309-320.

Liu, D.S.; Chiou, D.Y. (2005): 2D infinite element modeling for elastostatic problems with geometric singularity and unbounded domain. *Comput. Struct.*, vol. 83, pp. 2086-2099

Liu, D.S.; Chiou, D.Y.; Lin C.H. (2004): A hybrid 3D thermo-elastic infinite element modeling for area-arrey package solder joints. *Finite Elem. Anal. Des.*, vol. 40, pp. 1703-1727.

Liu, D.S.; Chiou, D.Y. (2004): Modeling of inclusion with interphases in hetero-

geneous material using the infinite element method. *Comp. Mater. Sci.*, vol. 31, pp. 405-420.

Liu, D.S.; Chen, C.Y.; Chiou, D.Y. (2005): 3D Modeling of a composite material reinforced with multiple thickly coated particles using the infinite element method. *CMES-Comp. Model. Eng.*, vol. 9, pp. 179-191.

Pahr, D. H.; Böhm, H. J. (2008): Assessment of mixed uniform boundary conditions for predicting the mechanical behavior of elastic and inelastic discontinuously reinforced composites. *CMES: Computer Modeling in Engineering & Sciences*, vol. 34, pp. 117-136.

Shen, C.H.; Springer G.S. (1977): Moisture absorption and desorption of composite materials. *Journal of Composite Materials*, vol. 10, no. 1, pp. 2-20.

Takashima, S.; Nakagaki, M.; Miyazaki, N. (2007): An elastic-plastic constitutive equation taking account of particle size and its application to a homogenized finite element analysis of a composite material. *CMES: Computer Modeling in Engineering & Sciences*, vol. 20, pp. 193-202.

Vaddadi, P.; Nakamura, T.; Singh, R.P. (2003): Inverse analysis for transient moisture diffusion through fiber reinforced composites. *Acta Mater.*, vol. 51, no. 1, pp. 177-193.

Vaddadi, P.; Nakamura, T.; Singh, R.P. (2003): Transient hygrothermal stresses in fiber reinforced composites: A heterogeneous characterization approach. *Compos. Part A*, vol. 34, no. 8, pp. 719-730.

Wong, E.H.; Teo, Y.C.; Lim, T.B. (1998): Moisture diffusion and vapor pressure modeling of IC packaging. *Proceedings of the 48th ECTC*, pp. 1372-1378.

Wong, E.H.; Rajoo, R.; Koh, S.W.; Lim, T.B. (2002): The mechanics and impact of hygroscopic swelling of polymeric materials in electronic packaging. *J. Electron. Packaging*, vol. 124, no, 2, pp. 122-126.

Ying, L.A. (1995): *Infinite Element Methods*. Peking University Press and Vieweg Publishing.